

# DETERMINATION OF RADIO WAVE PROPAGATION CONDITIONS IN THE ATMOSPHERE OF HANOI USING THE METEOROLOGICAL DATA

*Chi Cong Pham*<sup>1</sup>, *Xuan Anh Nguyen*<sup>2</sup>, *Hoai Trung Tran*<sup>3</sup>

## Abstract

This article uses the data of radio occultation and the radiosonde data to determine radio refractive index and wave propagation conditions in the atmosphere of the Hanoi area. The content of this article uses the data of radio occultation in 2014-2016 and the radiosonde data in 2016-2018, showing that the radio refractive index tends to decrease with altitude, the maximum average value of radio refractivity is 370 N-units, the largest radio refractivity difference between years is not more than 11 N-units, at high altitudes the radio refractivity value is close to the value at standard model of the ITU-R while at a small altitude the difference between the model value and the observed value is up to 60 N-units, the vertical gradient of refractivity and the effective earth radius coefficient is independent with altitude. Based on radio refractivity, it is possible to determine tropospheric delay, which is input data for problems such as satellite positioning, altimetry satellite and under-the-horizon radar.

## Index terms

Wave propagation condition, radio refractive index, refractivity gradient, k-factor, radiosonde balloon, radio occultation, meteorological data.

## 1. Introduction

Radio propagation in the troposphere is affected by the atmospheric refractive index or radio refractive index. Due to the heterogeneous propagation medium, according to Snell's law, the wave rays are deflected when passing through layers with different refractive indices [1]. It has been proved that the path of the electromagnetic wave is bent due to inhomogeneous spatial distribution of the refractive index, causing adverse effects such as multipath fading and interference, attenuation due to diffraction on the terrain obstacles or so called radio holes [2]. These effects significantly weaken radio communications, navigations, and radar systems. It is a position error in navigation and navigation systems, alters the angle of incidence in terrestrial communication systems,

---

<sup>1</sup> Vietnam Research Institute of Electronics, Informatics, and Automation (VIELINA), Hanoi, Vietnam

<sup>2</sup> Institute of Geophysics, VAST (IGP-VAST), Hanoi, Vietnam

<sup>3</sup> University of Transport and Communications (UTC), Hanoi, Vietnam

and changes the radar system's coverage. For line-of-sight communication systems, earth curvature and radio refraction affect the minimum antenna height and communication path distance; the effects of refraction are mainly in the first Fresnel zone. Due to atmospheric refraction phenomena such as super-refraction, ducted refraction can propagate waves over long distances. The transmission of tropospheric scattering waves, when electromagnetic waves encounter a medium with the radio refractive index heterogeneity and a change close to the wavelength, is also studied for applications in military communications.

Research on the refractive index is applied in using a satellite navigation system [3]. Accordingly, the troposphere causes signal delay, affecting positioning errors from 2.5-25 m (this does not take into account the wave direction that changes when  $N$  changes on the transmission line). An atmospheric model or direct observation data of the refractive index is required to correct this troposphere error [4]. By obtaining refractive index data from radiosonde balloon data, cosmic data will improve accuracy when determining the receiver's position in the satellite positioning problem. Due to the direct data from Hanoi, the accuracy is higher than using the global average model of ITU-R.

The tropospheric refractive index data also applies to satellite altimetry. Today satellite altimetry such as Sentinel is a powerful and fascinating Earth Observation technique that is of great importance in several applications such as measuring topographic elevation on the ground, studying level changes such as mean sea level (an important indicator of climate change), observing the melting of continental ice sheets. The article [5] presents an overview of the effect of the troposphere on the signal of the satellite altimetry, that is, the tropospheric Path Delay (PD) and the corresponding corrections. The requirement for refractive index (to determine tropospheric delay) is very high to ensure the requirements of the growing applications of satellite altimetry from 0.01-0.03 m. Having the correct rule of refractive index in Hanoi improves the correction of satellite altitude data here. In addition to the above applications, other applications are using atmospheric refractive index such as transmitting waves using radar below the horizon; the problem of determining the orbital position of the satellite from the ground station; problems in atmospheric and climate physics such as turbulent motion in the atmosphere, atmospheric microphysics, radiation balance studies, etc.

When considering the radio wave propagation conditions in the atmosphere, first, it is necessary to determine the radio refractive index and its spatial distribution, which is the fundamental parameter that must be the foundation for the researches about future transmission conditions. The radio refractive index can be determined by two methods of direct measurement and indirect measurement. The indirect measurement method through atmospheric parameters such as pressure, temperature, and humidity has the advantage of determining the refractive index in a wide range, using previous remote sensing results by satellites, radiosonde balloon, ... although the accuracy is not equal to the direct method by refractometer [6], [7]. The indirect measurement method is used in this research content. Research results on radio refractive index models are shown in

different versions of ITU-R recommendation and the last one, No. P.453-14 [8]. Some experimental research results determine the radio refractive index by indirect methods as in [9], [10], [11], or using radiosonde balloon data to determine the range of variation of refractive index and k-factor [12], the study of ducted refraction conditions [13] and study of anomalous propagation conditions affecting weather radars [14].

Hanoi area is located around latitude 21.01°N and longitude 105.80°E, with a tropical monsoon climate. The article shows the accuracy of the ITU-R refractive index model and the radio wave propagation conditions in the atmosphere of Hanoi area, using the radio occultation data of the COSMIC satellite in 2014-2016 simultaneously and radiosonde balloon data for the years 2016-2018 based on determining the radio refractive index by indirect method.

## 2. Theoretical background

### 2.1. Determination of atmospheric parameters

The atmospheric radio refractive index  $n$  is defined as the ratio of the propagation speed of an electromagnetic wave in a vacuum (or free space)  $c_0$  to the speed of wave propagation in a matter medium  $c$  according to the formula [1]:

$$n = \frac{c_0}{c} \quad (1)$$

The radio refractive index  $n$  has a value very close to 1, so in practice, radio refractivity  $N$  is often used. It is calculated through  $n$  according to the formula [7], [8]:

$$n = 1 + N \cdot 10^{-6} \quad (2)$$

The radio refractivity  $N$  can be determined through pressure, temperature, and humidity according to the formula [7], [8]:

$$N = 77.6 \frac{P}{T} - 5.6 \frac{e}{T} + 3.75 \cdot 10^5 \cdot \frac{e}{T^2} \quad (\text{N-units}) \quad (3)$$

where  $P$  is total atmospheric pressure (hPa),  $e$  is water vapor pressure (hPa),  $T$  is absolute temperature (°K).

The results in [7] have shown that, assuming the relative humidity is 60%, the pressure is 1013 mbar and there is no error in the equation for  $N$ , equation (3), then the measurement error of  $N$  from surface weather observations increases with temperature from  $\pm 0.38$  N-units (-50°C) up to  $\pm 2.83$  N-units (+40°C) with errors in pressure ( $\pm 1$  mbar), temperature ( $\pm 0.1$ °C), relative humidity ( $\pm 1\%$ ).

The vapor pressure  $e$  (hPa) can be calculated through the relative humidity  $H$  (%) and the saturated vapor pressure  $e_s$  (hPa) according to the formula [8]:

$$H = 100 \cdot \frac{e}{e_s} \quad (4)$$

According to Recommendation ITU-R No. P.453 [8], the saturated vapor pressure  $e_s$  (hPa) depends on the Celsius temperature  $t$  ( $^{\circ}\text{C}$ ) and the total atmospheric pressure  $P$  (hPa) according to the formula:

$$e_s = 6.1121 \cdot EF \cdot \exp\left[\frac{(18.678 - t/234.5)t}{t + 257.14}\right] \quad (5)$$

$$EF = 1 + 10^{-4}[7.2 + P \cdot (0.0320 + 5.9 \cdot 10^{-6} \cdot t^2)] \quad (6)$$

Also in [8], the reference profile used to calculate the value of the radio refractivity  $N_s$  at the earth's surface according to  $N_0$  is as follows:

$$N_s = N_0 \cdot \exp\left(-\frac{h_s}{h_0}\right) \quad (7)$$

where  $h_s$  (km) is the surface elevation above sea level.  $N_0$  and  $h_0$  are reference values of refractivity and altitude, which can be determined statistically for different climates. For reference purposes a global mean of the height profile of refractivity may be defined by  $N_0 = 315$  N-units,  $h_0 = 7.35$  km.

Wave rays when traveling in the troposphere of the atmosphere will be bent due to the phenomenon of refraction, the curvature of the wave ray is highly dependent on vertical gradient of the radio refractive index. The curvature of the wave ray has a positive value when the atmospheric refractive index decreases with altitude ( $dn/dh < 0$ ), the wave-ray trajectory has a downward concave surface and is called positive refraction. The curvature of the wave ray has a negative value in the opposite case ( $dn/dh > 0$ ), the wave-ray trajectory has an upward concave surface and is called negative refraction. The case if  $dn/dh$  is constant then the ray trajectory will be an arc [1], [7].

For the effect of atmospheric refraction, the commonly used method considers the wave ray propagating along a straight path not on the spherical surface of radius  $a$  but on a hypothetical sphere of radius  $R_e$ . The effective earth radius coefficient  $k$  ( $k$ -factor) is defined as the ratio of the effective radius  $R_e$  or the radius equivalent to the actual radius of the earth  $a$ ,  $k = R_e/a$ . Then the condition to switch the straight wave ray model is approximated by the formula [7]:

$$\frac{1}{ka} = \frac{1}{a} + \frac{dn}{dh} = \frac{1}{R_e} \quad (8)$$

where  $a$  is the actual radius of the earth, and  $R_e$  is the effective radius of the earth.

Thus, from (8) the effective earth curvature  $1/R_e$  when the wave passes through the lower layer of the earth's atmosphere, depends on the rate of change of the atmospheric refractive index with altitude. Taking the actual radius of the earth  $a \approx 6370$  km, the coefficient  $k$  is approximately calculated according to the formula [12], [15]:

$$k \approx \frac{1}{1 + \left(\frac{dN}{dh}\right)/157} = \left(1 + \frac{G}{157}\right)^{-1} \quad (9)$$

where  $G = dN/dh$  is the variation of radio refractivity with altitude or vertical gradient of radio refractivity, at the earth's surface there is  $G \approx -39$  N-units/km, then  $k \approx 4/3$  wave rays will propagate under normal refraction conditions or standard atmosphere.

Because atmospheric pressure and water vapor decrease rapidly with altitude, while temperature decreases slowly with altitude, so the radio refractive index depends on altitude and usually decreases with increasing altitude. When studying ducting refraction [1], [7], [8], the modified refractivity is called the refractive modulus, denoted by  $M$  (M-units) in the flat earth model; parameter  $M$  depends on both  $N$  (N-units) and altitude  $h$  (km). The refractive modulus  $M$  is used in computer ray-tracing software to analyze the phenomenon of ducting refraction. Other parameters are also used, such as  $A$ ,  $B$  also calculated from  $N$  for radio meteorology [7].

### 2.2. Effect of atmospheric parameters on wave propagation

The curve shows the relationship between  $k$  and  $G$ , according to formula (9), as shown in Fig. 1. At  $G = -39$  N-units/km,  $k = 4/3$  is the average atmospheric condition of the earth's surface. That's why called standard atmosphere or normal atmosphere. With  $G = -157$  N-units/km,  $k = \infty$ , then the curvature of the wave ray is equal to the real curvature of the earth; the wave ray trajectory is parallel to the spherical ground. In the case of  $G < -157$  N-units/km ( $k < 0$ ), the ray spreads, the radio waves are "trapped" like waveguides in the space between the earth's surface and/or the layers in the lower atmosphere. The curvature of the wave rays is greater than the real curvature of the earth. When  $G > -157$  N-units/km ( $k > 0$ ), the ray curvature is always less than the real curvature of the earth.

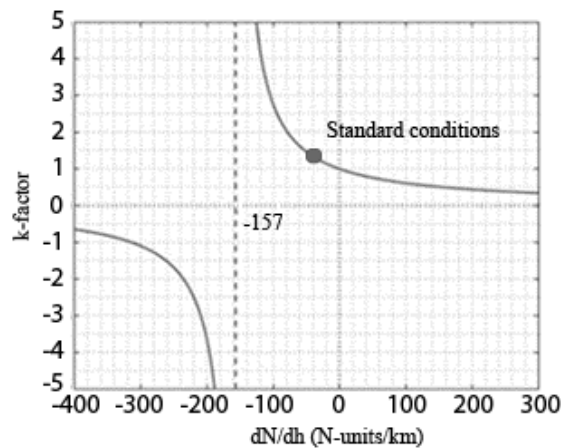


Fig. 1. The dependence between the effective earth radius coefficient and the variation of radio refractivity with height

The corresponding values of  $G$  and  $k$  commonly used to compare each other are  $G = 314$  ( $k = 0.33$ ),  $157$  ( $0.5$ ),  $0$  ( $1$ ),  $-157$  ( $\infty$ ),  $-314$  ( $-1$ ). Otherwise, the  $k$  and  $G$  values will be  $k = 1$  ( $G = 0$ ),  $4/3$  ( $-39$ ),  $2$  ( $-79$ ),  $\infty$  ( $-157$ ),  $< 1$  ( $> 0$ ), respectively.

Since the atmospheric parameters are pressure, temperature and humidity constantly change, resulting in a time-varying coefficient  $k$  (or  $G$ ). Fig. 2 shows wave propagation in the atmosphere with different  $k$  coefficients, specifically with  $k = 1$ , that is, no atmospheric refraction, straight wave propagation;  $k > 1$ , the wave has a downward concave surface with an increasing curvature as the  $k$  increases and is smaller than the actual curvature of the earth;  $k < 1$ , the wave ray has an upward concave surface [1], [16].

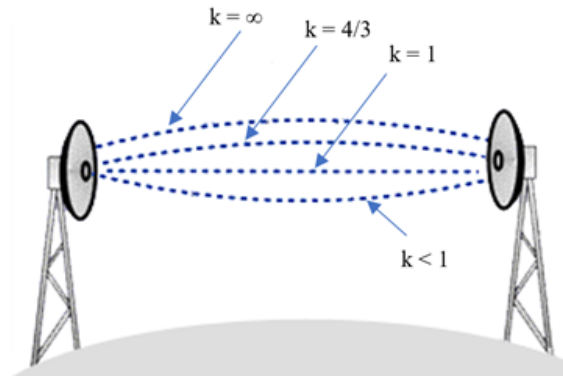


Fig. 2. Wave rays are bent under different atmospheres conditions (wave propagation with different  $k$ -factors)

The factor  $k$  indicates that the state of the atmosphere affects the trajectory of the ray and is often used to classify different types of refraction [17], [18]. These are sub-refraction, standard refraction, super-refraction, and ducting refraction. Specifically as follows:  $k = 4/3$ , propagating in standard or normal atmospheric conditions, with the curvature of the ray less than the actual curvature of the earth;  $0 < k < 4/3$ , sub-refraction conditions, wave-ray curvature less than in normal atmospheric conditions, or even concave upward ( $k < 1$ ,  $G > 0$ );  $+\infty > k > 4/3$ , super-refractive condition, the wave ray is bent downward to the ground and reflected on the ground with the curvature of the wave being more significant than the curvature when traveling in the standard atmosphere, but still less than the actual curvature of the earth;  $k = \infty$ , the wave's trajectory is parallel to the spherical ground, the curvature of the wave is equal to the actual curvature of the earth so that it can be propagated beyond the horizon;  $-\infty < k < 0$  in ducted refraction conditions, the curvature of the wave rays is greater than the actual curvature of the earth.

The ITU-R recommendations indicate that the coefficient  $k$  is generally in the range  $4/3 > k > 0.42$  [12]. In the range  $4/3 > k > 0.4$ , based on the  $k$  coefficient, it is possible to know how the wave propagation conditions are with weather and terrain [16], [19], as shown in Table 1.

An analytic study for the effect of antenna height on line-of-sight VHF/UHF communications coverage distance [19], show that with the coefficient  $k = 4/3$  having the most significant coverage,  $k = 0.45$  has the smallest coverage, with values of  $k$  in the range  $0.45 < k < 4/3$  will have a coverage area proportional to the  $k$  and lie between the two

Table 1. *k*-factor guide

<b>k-factor</b>	<b>Propagation</b>	<b>Weather</b>	<b>Terrain</b>
4/3	perfect	standard atmosphere	temperate zone, no fog
1 - 4/3	ideal	no surface layers, fog	dry, mountainous, no fog
2/3 - 1	average	substandard, light fog	flat, temperate, some fog
1/2 - 2/3	difficult	surface layers, ground fog	coastal
0.4 - 1/2	bad	fog moisture, over water	coastal, water, tropical

above coverage areas. This result is the same as in the ITU-R No. P.530 recommendation [20] based on the transmission path measurements in the temperate continental climate [21], when considering the effect of the coefficient  $k_e$  on the propagation distance in the line-of-sight communication system, which is the range  $1 > k_e > 0.5$ , the propagation distance is proportional to the coefficient  $k_e$ . With  $k_e$  defined as the value of  $k$ , which is exceeded 99.99% of the time.

Thus, by determining the coefficient  $k$ , the atmospheric refraction pattern and the direction of the wave can be determined. Especially in most cases of  $k$  ( $0 < k < 4/3$ ), the coverage areas propagation characteristics can be predicted in different weather and terrain conditions.

### 3. Materials and methods

A radiosonde balloon is a type of balloon used to carry equipment that measures various atmospheric parameters and transmits them by radio to a ground receiver. Modern radiosondes measure or calculate the following variables: altitude, pressure, temperature, relative humidity, wind (both wind speed and wind direction), cosmic ray readings at high altitude and geographical position (latitude/longitude). The balloon can be tracked by radar, radio waves, or using a global positioning system to obtain wind data. The height of the balloon can be adjusted by the amount of air injected into the balloon. The balloon can reach a height of 25-35 km or more depending on weather conditions; the range can reach hundreds of km depending on wind speed. The time of day when the balloon is released, the number of atmospheric observation parameters and data sharing complies with the World Meteorological Organization regulations (WMO).

In Hanoi, the radiosonde balloons are released twice a day at 00Z (+7GMT) and 12Z (+7GMT). Day data collected and saved are two files with CSV format corresponding to the two above times. Daily data is stored in the folder of each month; month data is stored in each year's folder. Statistics for the period 1990-2020 are shown in Table 2. This is the meteorological observation data of Noi Bai airport (code VVNB), which can be found in [22].

In each data file are records containing information about altitude (*HGHT*), pressure (*PRES*), temperature (*TEMP*), relative humidity (*RHLH*), and some other meteorological parameters such as dew point temperature (*DWPT*), wind direction (*DRCT*), ... altitude

Table 2. Radiosonde balloon data collection

Year	File	Year	File	Year	File	Year	File
1990	358	1998	0	2006	30	2014	28
1991	142	1999	465	2007	41	2015	32
1992	218	2000	148	2008	41	2016	698
1993	544	2001	47	2009	34	2017	697
1994	0	2002	39	2010	35	2018	678
1995	0	2003	25	2011	31	2019	420
1996	0	2004	22	2012	35	2020	655
1997	0	2005	24	2013	33		

from the surface to 20 km, which includes many different observation heights and the unfixed distance between the heights. The data is processed and converts to 0.1 km spaced elevations; 0.1; 0.2; 0.3; ... to 20 km by the moving average method. The formula calculates the radio refractivity at each equally spaced height in (3, 4, 5, 6) from pressure, temperature, and humidity parameters.

The technique of using Global Navigation Satellite System (GNSS) receivers at Low Earth Orbit (LEO) to measure GNSS signals to study the atmosphere based on movement relative between LEO and GNSS satellites, as a result, the obtained GNSS signal can trip across the earth's atmosphere in the occultation according to the layers at different heights, which is called radio occultation [23], [24]. Several parameters such as density, temperature, pressure, and water vapor can be calculated through radio occultation. Currently, many LEO low-altitude satellites are launched into orbit to collect occultation data such as GPS/MET (USA), CHAMP (Germany), SAC-C (Argentina), Orsted (Denmark), ...

COSMIC/FORMOSAT-3 is a system consisting of meteorological observation satellites, ionosphere and climate (Constellation Observing System for Meteorology, Ionosphere and Climate-1) also called COSMIC1, is a cooperative space program between Taiwan (China) and the US launched in 2006 with the launch of 6 satellites into low-earth orbit. Currently, this program has completed its mission (in 2020) and replaced by COSMIC/FORMOSAT-7 or COSMIC2. The COSMIC satellite tomography data includes many different levels, along with many types of data at each level depending on how the data is processed. The moisture profile data at level 2 used in this paper is from the COSMIC/FORMOSAT-3 satellite distributed by CDAAC, requiring registration [25]. The data is collected for 2006-2020 using Curl (Client URL), a tool used to check the connection to the URL and is often used to transmit data. The time from 2006-2014 (112th day 2006 to 120th day 2014) is COSMIC2013 data, and from 2014-2020 (121st day 2014 to 116th day 2020) is COSMIC data.

Occultation data (tar file - file format on Unix-based systems) is stored in each year's directory with a total capacity of nearly 85 GB. In one data file, there are many moisture profile files (wetPrf) from different satellites. Statistics of data files in years, and the corresponding number of moisture profile files are as shown in Table 3.



Table 3. Radio occultation data collection

Year	Data File	Moisture Profile	Year	Data File	Moisture Profile
2006	243	281245	2014	364	429029
2007	365	758682	2015	361	251014
2008	364	718207	2016	361	246530
2009	365	403802	2017	352	126688
2010	365	590234	2018	343	96986
2011	364	416939	2019	202	48729
2012	366	516079	2020	32	2193
2013	365	598377			

The moisture profile data is in the format of netCDF [26]. It is an open, self-describing data format that allows the storage of multidimensional data. Parameter data included in the moisture profile include: altitude above sea level (*MSL\_alt*) from 0.1 km to 39.9 km, the distance between each data layer is 0.1 km; longitude (*Lat*); latitude (*Lon*); pressure (*Pres*), temperature (*Temp*), relative humidity (*Vp*) and some other data fields. The radio refractivity (*Ref*) can be calculated in equations (3, 4, 5, 6). The number of days with radio occultation data in the Hanoi area is shown in Table 4. This is from calculating within a radius of 2° at the location with latitude 21.01°N and longitude 105.80°E.

Table 4. Occultation data collection in the Hanoi area

Year	No. of days	Year	No. of days	Year	Day	Year	No. of days
2006	-	2010	-	2014	87	2018	34
2007	-	2011	-	2015	86	2019	20
2008	-	2012	-	2016	100	2020	-
2009	-	2013	-	2017	48		

The acquisition of radiosonde balloon data and occultation data can be performed by a program running in the background, operating continuously, automatically fetching data each time new data is detected, and storing it in local memory according to the folders of each year, month, and day. This article uses COSMIC data for 2014-2016 because there are many occultation data in the Hanoi area and 2016-2018 radiosonde balloon data due to incomplete data in 2019 and 2020 (in 2019, there is no data available on June and August, 2020 has missing multi-day figures). Based on the collected data, the radio refractive index according to atmospheric parameters and spatial structure of the radio refractive index can be calculated, thereby determining the variation of radio refractivity with altitude *G* and the effective earth radius coefficient *k*, that is the basis for determining radio wave propagation characteristics in the atmosphere of Hanoi area.

#### 4. Results and Discussion

Based on radiosonde balloon data, calculating the average radio refraction in the last five years from 2016-2020 results is shown in Table 5. The radiosonde balloon

method showed that for 2016-2018, the average radio refractivity was in the range of 38-370 N-units. The difference of radio refractivity values between years is little small. Specifically, the highest difference in maximum radio refractivity values is not more than 1 N-units, and the highest difference in minimum radio refractivity values is not more than 3 N-units. Generally, for 2016-2020, the radio refractivity is still in the range of 38-370 N-units, the difference in minimum values are not more than 3 N-units, and the difference in maximum values are not more than 4 N-units.

Table 5. Range of average radio refractivity of radiosonde balloon data

Value	Radio Refractivity (N-Units)				
	2016	2017	2018	2019	2020
Min (20.0 km)	40.71	40.83	38.05	40.68	40.90
Max (0.1 km)	368.49	369.19	368.89	365.84	366.23

The radio refractivity is determined based on occultation data in Table 4, giving the results for the range of average radio refractivity values for the years 2014-2019 with tomographic data in the Hanoi area as shown in Table 6.

Table 6. Range of average radio refractivity of occultation data

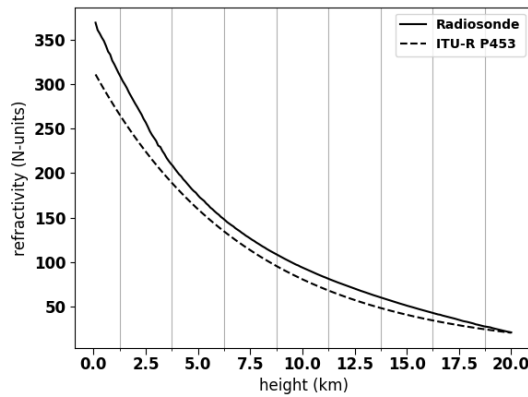
Value	Radio Refractivity (N-Units)					
	2014	2015	2016	2017	2018	2019
Min (39.9 km)	0.91	1.10	0.92	0.91	0.89	1.32
Max (0.1 km)	367.62	363.35	356.65	353.23	330.39	346.03

In the COSMIC method, the highest average radio refractivity is 368 N-units. At an altitude of nearly 40 km, the radio refractivity value gradually decreases to 0 N-units, The largest difference in radio refraction maximum values between 2014-2016 are not more than 11 N-units; if the years 2017-2019 are included, this value is up to 38 N-units because 2017-2019 have little occultation data at low altitudes. Because the radio refractivity has a significant value at low altitudes, so the highest value of radio refractivity in the years 2017-2019 is low. The difference in the lowest value of refractivity between the years is not more than 1 N-units.

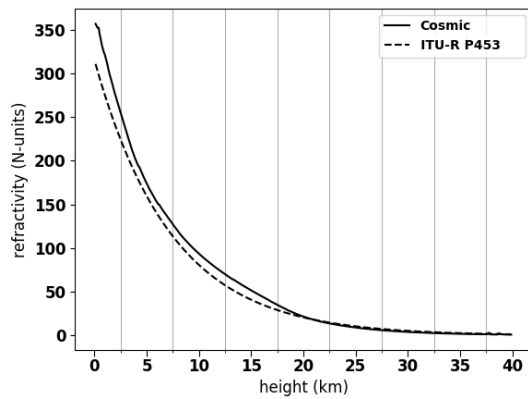
From Table 5 and Table 6, in 2016-2019, the maximum average radio refractivity by the radiosonde balloon method is almost always greater than that of the radio occultation method. Specifically, in 2016 the difference in the maximum value of radio refractivity was 11.84 N-units. The difference of measured values in the following years is as follows: 15.96 N-units (2017), 38.5 N-units (2018), 19.81 N-units (2019). Calculating average maximum refractivity value over the years of using data for surveying for radiosonde balloon (2016-2018) and radio occultation (2014-2016), the difference in average maximum value is 6.32 N-units.

Calculation results depend on radio refractivity according to height as shown in Fig. 3,

with a solid line (above) is the result of indirect measurement of radio refractivity, dashed line (below) is the calculated value according to the standard model of ITU-R, according to formula (7). From the results in Fig. 3, it can be seen that: The curve showing the dependence of radio refraction on altitude in two methods of the radiosonde balloon and radio occultation is quite similar. They are almost similar, and slightly larger than the calculated value according to the ITU-R model, the radio refractivity decreases with altitude. The radio refractivity is close to the model value for high altitudes. At low altitudes, the difference is quite clear.



(a) radiosonde balloon data



(b) cosmic data

Fig. 3. Observed refractivity (solid line) and refractivity according to ITU-R model (dashed line)

The difference between the observed radio refractivity value and the value in the ITU-R model as shown in formula (7) representing the deviation from the reference value is calculated as follows:

$$\Delta N_{hs} = N_h - N_s \quad (\text{N-units}) \quad (10)$$

where  $N_h$  (N-units) is the observed refractivity by indirect method at the height  $h$  (km),  $N_s$  (N-units) is the refractivity calculated according to the ITU-R model.

The calculation of the absolute difference between the observed radio refractivity value and the ITU-R model value results in Fig. 4. The results show that the difference is not uniform and varies with altitude. The low-altitude atmosphere is the most significant at less than 60 N-units. Over 3.75 km, this difference is less than 20 N-units, at altitudes above 17.5 km, this difference is less than 10 N-units, at altitudes above 20 km, the difference is a small value at  $\pm 0$  N-units, which means that the observed value and the model value are almost similar.

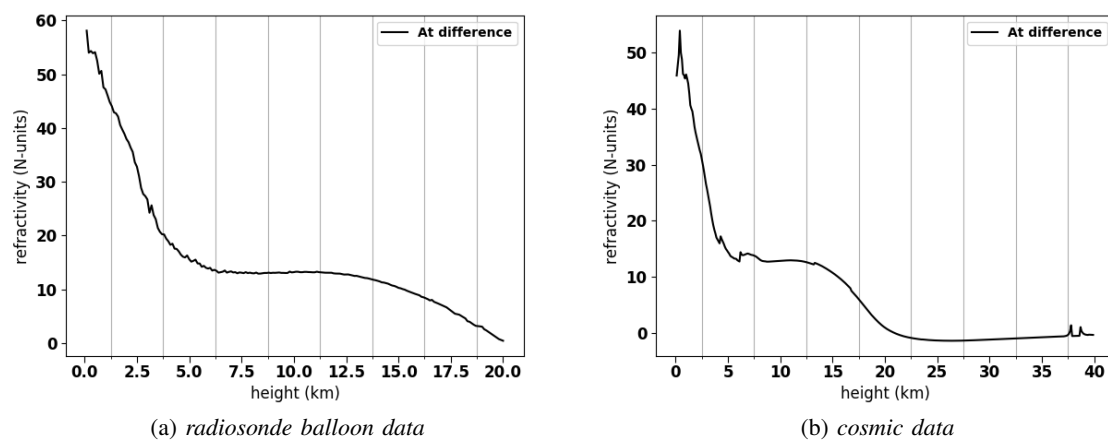


Fig. 4. The difference between the observed refractivity and the refractivity according to the ITU-R model

The difference between radio refractivity values measured by radiosonde balloon method and radio occultation method is determined as follows:

$$\Delta N_{rc} = N_r - N_c \quad (\text{N-units}) \quad (11)$$

where  $N_r$  (N-units) is the radio refractivity determined by the radiosonde balloon method,  $N_c$  (N-units) is the radio refractivity calculated by the radio occultation method.

Determination of the absolute difference between the radio refraction values observed by the radiosonde balloon method and the radio occultation method gives the results in Fig. 5. It is found that the radio refraction value in the radiosonde balloon method in most altitudes is larger than that in radio occultation. Only around the altitudes of 2.5 km, 7.5 km and 15.0 km, the radio occultation value is greater than the radiosonde balloon value, but not by much less than 2 N-units. The maximum value difference of the two measurements is at less than 13 N-units. Meanwhile, the largest mean difference in radiosonde balloon and radio occultation methods is 6.32 N-units. This is explained because in 2014, 2015, the radio refractivity did not have the maximum value at small

altitudes, so the absolute difference for each height in the two measurements is different. At altitudes below 6.25 km, the value difference of the two measurements seems to be higher at lower altitudes. At low altitudes, the difference is shown more.

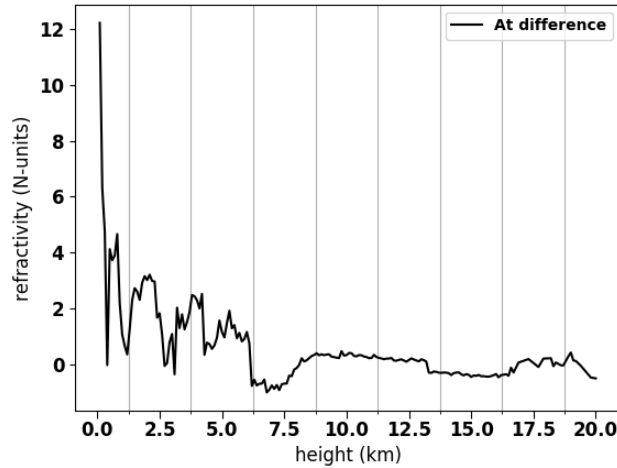


Fig. 5. The difference between refractivity observed by radiosonde balloon and radio occultation method

Calculating the variation of radio refractivity with altitude (gradient) gives the result shown in Fig. 6. Unlike the radio refractivity, vertical gradient of refractivity  $G$  is independent of altitude. However, in general, the gradient tends to increase with altitude. In the range of fewer than 10 km, radio refractivity varies significantly with altitude, thus affecting many of the trajectories of the wave.

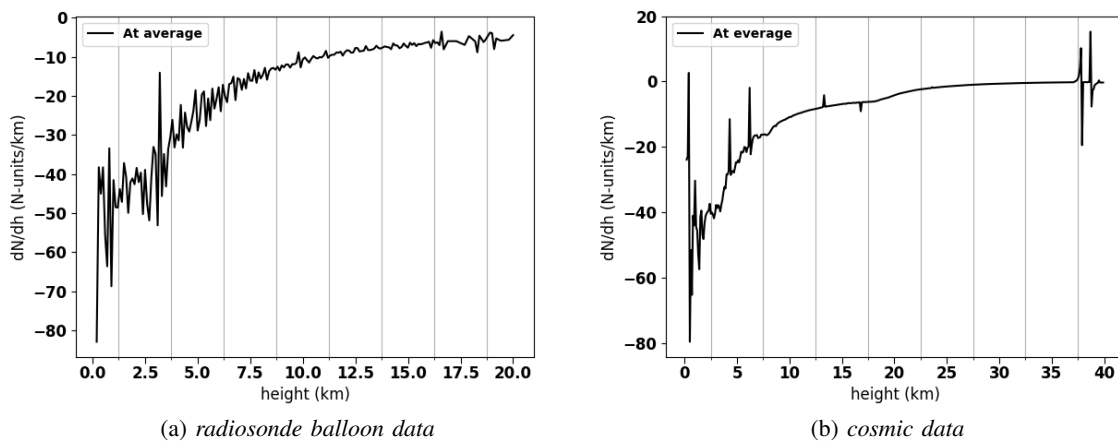


Fig. 6. Variation of radio refractivity with altitude

Specifically, at altitudes below 3.75 km, the value of  $G$  changes much around  $G = -40$  N-units/km, in the range of 3.75-10 km, the value of  $G$  changes less and at  $G > -40$  N-units/km. In the range from 10-35 km, the  $G$  value changes little, then the propagation direction of the wave is stable. The variation of radio refractivity with altitude has an unusual change at an altitude of 35-40 km. This is related to the phenomenon of temperature inversion (also called thermal inversion), when the temperature of the upper atmosphere is higher than the temperature of the lower atmosphere, leading to an increase in the radio refractive index with altitude and an abnormal change in the value of  $G$ . This phenomenon usually occurs with high frequency in winter when the air is stable, the night is prolonged and cold air comes in.

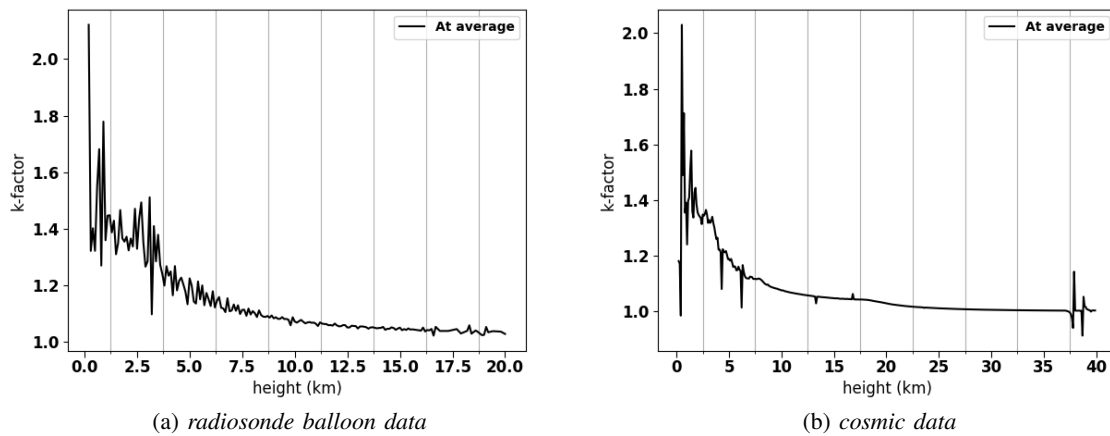


Fig. 7. Variation of effective earth radius coefficient

The effective earth radius coefficient  $k$  is used to determine the propagation direction of waves in the atmosphere. As shown in Fig. 7, the factor  $k$  is also independent of height. Generally,  $k$  tends to decrease with altitude. The effective earth radius coefficient always has a value of  $k > 0$ , as a result, the waves will propagate under sub-refraction conditions or in the super-refractive conditions, the wave bends downward with  $k > 1$ , upward with  $k < 1$  and does not occur the ducting refraction corresponding to the case  $-\infty < k < 0$ . Wave propagation in super-refractive conditions is because Hanoi area has tropical monsoon climate, there are storms and thunderstorms every year, and super-refraction usually occurs before each storm [27], so there is super-refraction during wave propagation. At an altitude of 10-35 km, the factor  $k$  does not change much in the range of 1.0-1.2, then the wave propagation is under ideal conditions and without a surface layer (as shown in Table 1), the wave ray can propagate further than no refraction.

Since the atmosphere radio refractive index is always greater and close to unity ( $>1$ ), the way-ray propagates more slowly in free space, which increases the delay in measurements and causes errors in locating use GNSS. The study of the troposphere delay will provide a way to compensate for this delay, helping to improve positioning

accuracy. The tropospheric delay is a function of the total refractivity  $N$  (N-units), which depends on the pressure  $P$  (mbar or hpa), the temperature  $T$  (K) and the relative humidity  $RH$  (%) or vapor component pressure  $e$  (mbar or hpa) along the path of the signal along with the receiver position.

The  $ZTD$  (Zenith Tropospheric Delay) or vertical delay can be calculated by integration of the total refractivity along the signal transmission path according to the formula as follows [28]:

$$ZTD = 10^{-6} \int_0^{\infty} N(h)dh = 10^{-6} \sum_{i=1}^{top} N_i \Delta s_i \quad (m) \quad (12)$$

where  $N_i$  (N-units) is the radio refractivity at the  $i$ -th level,  $\Delta s_i$  is the distance (m) between the  $i$ -th and  $i+1$  level.

From  $ZTD$ , it is possible to determine the delay in different slant directions by a mapping function, which is dependent on both elevation and azimuth [29].

With the data of 02/2016 of the radiosonde balloon, the calculated results of the zenith delay are shown in Fig. 8. The smallest tropospheric delay (the zenith delay) is a variable quantity; most of the time it is above the level 2.12 m, while calculated according to the ITU-R model, this delay is unchanged, at less than 2.12 m (horizontal dashed line). This delay change is one of the causes that makes the results of the positioning measurement also to change and cause errors.

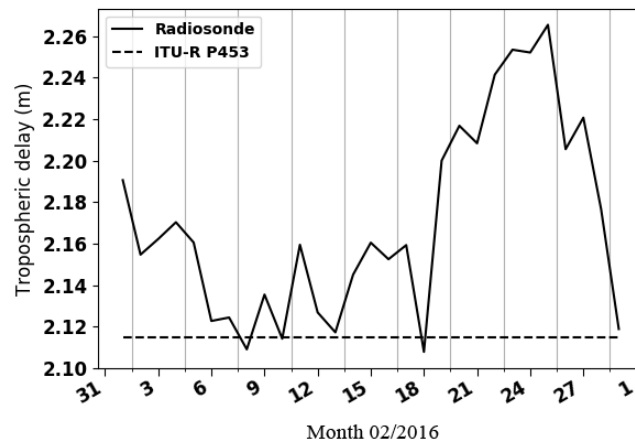


Fig. 8. Variation of zenith delay using radiosonde balloon data. The below horizontal dashed line is from the ITU-R model

Radiosonde balloon data is an in-situ measurement, which is one of the most practical sources of data for the most accurate refractive index calculations. Therefore, we suggest using this data source when it is necessary to correct for the effect of the tropospheric delay. Its limitation applies to a small range; when required in other locations where

no radiosonde balloon data are available, COSMIC data or alternative models are used. COSMIC data allows the survey of radio refractive index over a wide range (countries, territories) with less precision. The data is limited (although there are 14 years of global data but the data for an area is not much; the statistical results are as shown in Table 4), specifically when observing the average radio refractivity value, the different value of the radio occultation method compared with the radiosonde balloon method in levels up to 13 N-units. Calculating the refractive index according to the ITU-R model allows it to be applied globally. However, its accuracy is less than the data of radiosonde balloons or COSMIC, so not applicable to the problem that needs tropospheric delay to be determined accurately to a few centimeters as in altimeter satellite applications.

The results here also show that the observed radio refractivity is much different from the ITU-R model value in the low-atmospheric range, i.e., the ITU-R model value is less accurate at low altitudes; this difference amounts to almost 60 N-units. The reason is that the state of the atmosphere is affected by geographical factors at low altitudes are more, so there is a difference in the refractive index value at low altitudes. Therefore, we propose to use in-situ measurements to obtain an accurate refractive index when studying wave propagation conditions in the atmosphere.

## 5. Conclusions

By simultaneously using balloon data and radio occultation data, this article has shown the main features of radio refractive index and radio wave propagation conditions in the atmosphere of Hanoi area, in addition, it is proposed to use in-situ measurement to obtain the radio refractive index accurately when studying wave propagation conditions in the atmosphere if these data are available.

## References

- [1] M. Trevor, *Microwave Radio Transmission Design Guide, Second Edition*. Artech House, 2009.
- [2] J. Lavergnat and M. Sylvain, *Radio Wave Propagation: Principles and Techniques*. John Wiley & Sons, 2000.
- [3] K. Malek, E. Mohamed, and N. Aboelmagd, *Multifunctional Operation and Application of GPS*, ch. GNSS Error Sources. IntechOpen, 2018.
- [4] I. Mouhannad and L. Vadim, "Algorithm for tropospheric delay estimation using genetic algorithm for calculating the coordinates of a stationary GNSS receiver," in *AIP Conference Proceedings 2318, 130002*, 2021.
- [5] J. M. Fernandes, C. Lázaro, and T. Vieira, "On the role of the troposphere in satellite altimetry," *Remote Sensing of Environment*, vol. 252, 2021.
- [6] R. E. McGovin, *A survey of the techniques for measuring the radio refraction index*. U. S. Department of Commerce, National Bureau of Standards, 1962.
- [7] B. R. Bean and E. J. Dutton, *Radio Meteorology*. National Bureau of Standards Monograph 92, U.S. Government Printing Office, 1966.
- [8] ITU-R, "The refractive index: Its formula and refractivity data," Recommendation No. P.453-14, International Telecommunication Union, 2019.
- [9] I. J. Etokebe, M. U. Kufre, and I. A. Ezenugu, "Determination of atmospheric effective earth radius factor (k-factor) under clear air in Lagos, Nigeria," *Mathematical and Software Engineering*, vol. 2, pp. 30–34, 2016.
- [10] E. U. Kingsley and A. Samuel, "Review of methodology to obtain parameters for radio wave propagation at low altitudes from meteorological data: New results for Auchi area in Edo state, Nigeria," *Journal of King Saud University - Science*, vol. 31, pp. 1445–1451, 2019.



- [11] G. Martin and K. Vaclav, "Atmospheric refraction and propagation in lower troposphere," *Electromagnetic Waves*, 2011.
- [12] T. J. Afullo, M. O. Adongo, T. Motsoela, and D. F. Molotsi, "Estimates of refractivity gradient and k-factor ranges for Botswana," *The Transactions of the S.A Institute of Electrical Engineers*, 2001.
- [13] S. Mentés and Z. Kaymaz, "Investigation of surface duct conditions over Istanbul, Turkey," *Journal of Applied Meteorology and Climatology*, vol. 46, pp. 318–337, 2007.
- [14] J. Bech, A. Sairouni, B. Codina, J. Lorente, and D. Bebbington, "Weather radar anaprop conditions at a mediterranean coastal site," *Physics and Chemistry of the Earth, Part B: Hydrology, Oceans and Atmosphere*, vol. 25, pp. 829–832, 2000.
- [15] C. A. Levis, J. T. Johnson, and F. L. Teixeira, *Radiowave Propagation : Physics and Applications*. John Wiley & Sons, 2010.
- [16] L. N. Tho, "Basic radio propagation & path engineering," *ECSE413B: Communications Systems II*, 2008.
- [17] L. W. Barclay, *Propagation of radiowaves*. Institution of Electrical Engineers, 2013.
- [18] A. T. Adediji, M. O. Ajewole, and S. E. Falodun, "Distribution of radio refractivity gradient and effective earth radius factor (k-factor) over Akure, South Western Nigeria," *J. Atmosp. Solar-Terrestrial Phys*, vol. 73, pp. 2300–2304, 2011.
- [19] A. E. A. K. Firas and H. A. Rasha, "An analytic study for the effect of antenna height on line-of-sight VHF/UHF communications coverage distance applied to Baghdad city," *Periodicals of Engineering and Natural Sciences*, vol. 7, pp. 1965–1976, 2019.
- [20] ITU-R, "Propagation data and prediction methods required for the design of terrestrial line-of-sight systems," Recommendation No. P.530-17, International Telecommunication Union, 2017.
- [21] L. Boithias and J. Battesti, "Protection against fading on line-of-sight radio-relay systems (in French)," *Ann des Télécomm*, vol. 22, pp. 230–242, 1967.
- [22] "Atmospheric Soundings - University of Wyoming, Department of Atmospheric Science." <http://weather.uwyo.edu/upperair/sounding.html>. Accessed on December 6, 2021.
- [23] Y.-H. Kuo, S. Sokolovskiy, R. A. Anthes, and F. Vandenberghe, "Assimilation of GPS radio occultation data for numerical weather prediction," *Special issue of Terrestrial, Atmospheric and Oceanic Science*, vol. 11, pp. 157–186, March 2000.
- [24] Y. A. Liou, A. G. Pavelyev, S. S. Matyugov, and O. I. Yako, *Radio Occultation Method for Remote Sensing of the Atmosphere and Ionosphere*. InTech, 2010.
- [25] "CDAAC: COSMIC Data Analysis and Archive Center - University Corporation for Atmospheric Research, UCAR Community Programs." <https://cdaac-www.cosmic.ucar.edu/cdaac/index.html>. Accessed on December 6, 2021.
- [26] "Network Common Data Form (NetCDF) - University Corporation for Atmospheric Research, UCAR Community Programs." <https://www.unidata.ucar.edu/software/netcdf>. Accessed on December 6, 2021.
- [27] S. Park and F. Fabry, "Estimation of near-ground propagation conditions using radar ground echo coverage," *Journal of Atmospheric and Oceanic Technology*, vol. 28, pp. 165–180, 2011.
- [28] S. Osah, A. A. Acheampong, C. Fosu, and I. Dadzie, "Evaluation of zenith tropospheric delay derived from ray-traced VMF3 product over the West African region using GNSS observations," *Advances in Meteorology*, 2021.
- [29] Q. Zhao, Y. Yao, W. Yao, and Z. Li, "Real-time precise point positioningbased zenith tropospheric delay for precipitation forecasting," *Scientific Reports*, 2018.

Manuscript received 22-07-2021; Accepted 30-11-2021. ■



**Chi Cong Pham** received a master's degree in Electronic Engineering in 2017, working at the Vietnam Research Institute of Electronics, Informatics and Automation. Main research directions are wave propagation, artificial intelligence, intelligent systems, and the Internet of Things (IoT). Email: phamchicong@gmail.com



**Xuan Anh Nguyen** received his doctorate in 2000, majoring in Physics, working at Institute of Geophysics, Vietnam Academy of Science and Technology. Main research directions on navigation, LIDAR, measurement, and lightning protection systems. Email: nxuananh05@gmail.com



**Hoai Trung Tran** got Bachelor degree in University of Transport and Communications (UTC) in 1997 and hold the post of lecturer at the University. He then got a Master degree from Hanoi University of Science and Technology (HUST) in 2000. In the period 2003 to 2008, he had concentrated on researching in the field of Telecommunication engineering and got his PhD at University of Technology, Sydney (UTS) in Australia. He is currently a lecturer at the UTC. His main research interests are digital signal processing (DSP), applied information theory, radio propagation, MIMO antenna techniques and advanced wireless transceiver design. E-mail: trungth@utc.edu.vn

## XÁC ĐỊNH ĐIỀU KIỆN LAN TRUYỀN SÓNG VÔ TUYẾN TRONG KHÍ QUYỂN KHU VỰC HÀ NỘI SỬ DỤNG SỐ LIỆU KHÍ TƯỢNG

*Phạm Chí Công, Nguyễn Xuân Anh, Trần Hoài Trung*

### Tóm tắt

Bài báo sử dụng số liệu cắt lớp vô tuyến và số liệu bóng thám không để xác định độ khúc xạ vô tuyến và điều kiện lan truyền sóng trong khí quyển khu vực Hà Nội. Nội dung nghiên cứu sử dụng số liệu cắt lớp vô tuyến các năm 2014-2016 và số liệu bóng thám không 2016-2018 chỉ ra độ khúc xạ vô tuyến có xu hướng giảm theo độ cao, giá trị độ khúc xạ vô tuyến trung bình cao nhất là 370 N-units, chênh lệch độ khúc xạ vô tuyến lớn nhất giữa các năm thường ở mức không quá 11 N-units, ở độ cao lớn giá trị độ khúc xạ vô tuyến gần giống so với giá trị ở mô hình chuẩn của ITU-R trong khi ở độ cao nhỏ chênh lệch giữa giá trị độ khúc xạ vô tuyến theo mô hình và giá trị quan sát được lên tới 60 N-units, giá trị độ khúc xạ vô tuyến và hệ số bán kính trái đất hiệu dụng được chứng minh là không phụ thuộc vào độ cao. Dựa vào độ khúc xạ vô tuyến có thể xác định độ trễ tín hiệu qua tầng đối lưu, là số liệu đầu vào cho các bài toán như định vị vệ tinh, vệ tinh độ cao, ra-đa dưới chân trời...